Tensor Fermi liquid parameters in nuclear matter from chiral effective field theory

J. W. Holt,[1] N. Kaiser,[2] and T. R. Whitehead[1]
[1]*Cyclotron Institute and Department of Physics and Astronomy, Texas A&M University, College Station, Texas 77843, USA*
[2]*Physik Department, Technische Universität München, D-85747 Garching, Germany*

(Received 2 January 2018; published 23 May 2018)

We compute from chiral two- and three-body forces the complete quasiparticle interaction in symmetric nuclear matter up to twice nuclear matter saturation density. Second-order perturbative contributions that account for Pauli blocking and medium polarization are included, allowing for an exploration of the full set of central and noncentral operator structures permitted by symmetries and the long-wavelength limit. At the Hartree-Fock level, the next-to-next-to-leading order three-nucleon force contributes to all noncentral interactions, and their strengths grow approximately linearly with the nucleon density up to that of saturated nuclear matter. Three-body forces are shown to enhance the already strong proton-neutron effective tensor interaction, while the corresponding like-particle tensor force remains small. We also find a large isovector cross-vector interaction but small center-of-mass tensor interactions in the isoscalar and isovector channels. The convergence of the expansion of the noncentral quasiparticle interaction in Landau parameters and Legendre polynomials is studied in detail.

DOI: 10.1103/PhysRevC.97.054325

I. INTRODUCTION

Fermi liquid theory [1–4] is widely used to describe the transport, response, and dynamical properties of nuclear many-body systems [5–13]. The key quantity in this theory is the quasiparticle interaction, defined as the second functional derivative of the energy with respect to the quasiparticle distribution function. For many years the primary focus of investigation has been the central part of the quasiparticle interaction and its associated Fermi liquid parameters, which are directly related to static properties of the interacting ground state such as the incompressibility, isospin-asymmetry energy, and magnetic susceptibility. The central terms include scalar operators in spin and isospin space, but more recently noncentral contributions [14,15] that couple spin and momenta have been studied together with their impact on the density and spin-density response functions of neutron matter [16–19]. Extending these results to nuclear matter with equal numbers of protons and neutrons and to systems with arbitrary isospin asymmetry will be needed to better understand neutrino transport and emissivity in neutron stars, proto-neutron star cooling [20], electron transport in neutron stars [21], the evolution of shell structure and single-particle states in nuclei far from stability [22,23], and nuclear collective excitations (spin and spin-isospin modes together with rotational modes of deformed nuclei) [24–26].

An important motivation of the present work is to provide microscopic guidance for the tensor forces employed in modern mean field effective interactions and nuclear energy density functionals. Including as well new estimates and uncertainties on the central Fermi liquid parameters, which are more directly related to nuclear observables, the present study will complement other recent efforts [27–32] to constrain energy density functionals from microscopic many-body theory. The importance of tensor forces in mean field modeling is a question of ongoing debate. While there is skepticism [33,34] that tensor forces can lead to a meaningful improvement in fits to nuclear ground state energies, there is strong evidence that the description of single-particle energies [22,23,35,36], beta-decay half-lives [37], and spin-dependent collective excitations [25,26] are systematically improved with the inclusion of tensor forces (for a recent review, see Ref. [38]). One of the main driving questions is the extent to which the effective medium-dependent tensor force in mean field models resembles the fundamental tensor component of the free-space nucleon-nucleon interaction arising from $\pi + \rho$ meson exchange. A main conclusion of the present work is that the proton-neutron effective tensor force is enhanced over the free-space tensor interaction due to three-body forces and second-order perturbative contributions. On the other hand, the proton-proton and neutron-neutron tensor forces are considerably smaller in magnitude. In addition, we find evidence for a large isovector cross-vector interaction that to our knowledge has not been previously studied in phenomenological mean field modeling of nuclei.

The quasiparticle interaction can be computed microscopically from realistic two- and three-body forces starting from the perturbative expansion of the energy density and taking appropriate functional derivatives with respect to the distribution functions. For nuclear or astrophysical systems with densities near or above that of saturated nuclear matter, it is essential to consider the effects of three-body forces. To date three-nucleon forces have been included in calculations of the central and exchange-tensor quasiparticle interaction in nuclear matter [39–44] and the full quasiparticle interaction in neutron matter [45]. In the present work our aim is to extend the calculations in Ref. [45] to the case of symmetric nuclear matter. This is a natural step before considering the more general case of isospin-asymmetric nuclear matter.

We take as a starting point a class [46–51] of realistic two- and three-body nuclear forces derived within the framework of chiral effective field theory [52–54]. The two-body force is treated at both next-to-next-to-leading order (N2LO) and N3LO in the chiral power counting, while the three-body force is only considered at N2LO. Although the inclusion of consistent three-body forces at N3LO [55,56] in the chiral power counting will be needed for improved theoretical uncertainty estimates [57–59], the present set of nuclear force models has been shown to give a good description of nuclear matter saturation [50,60], the nuclear liquid-gas phase transition [61], and the volume components of nucleon-nucleus optical potentials [62,63] when used at second order in many-body perturbation theory. In addition to the order in the chiral expansion, the resolution scale (related to the momentum-space cutoff in the nuclear potential) is varied in order to assess the theoretical uncertainties.

The paper is organized as follows. In Sec. II we review the derivation of the quasiparticle interaction and associated Fermi liquid parameters from microscopic nuclear two- and three-body interactions. We present a general method to extract the central and noncentral components of the quasiparticle interaction from appropriate linear combinations of spin- and isospin-space matrix elements. We also benchmark the numerical calculations of the second-order contributions to the quasiparticle interaction against semianalytical results for model interactions of one-boson exchange type. In Sec. III we present analytical expressions for the Landau parameters arising from the leading N^{2}LO chiral three-body force together with numerical results for the second-order contributions from two- and three-body forces. We end with a summary and conclusions.

II. QUASIPARTICLE INTERACTION IN SYMMETRIC NUCLEAR MATTER

A. General structure of the quasiparticle interaction

The quasiparticle interaction in symmetric nuclear matter has the general form [15]

$$\mathcal{F}(\vec{p}_1,\vec{p}_2) = \mathcal{A}(\vec{p}_1,\vec{p}_2) + \mathcal{A}'(\vec{p}_1,\vec{p}_2)\vec{\tau}_1\cdot\vec{\tau}_2, \tag{1}$$

where

$$\begin{aligned}\mathcal{A}(\vec{p}_1,\vec{p}_2) = {}& f(\vec{p}_1,\vec{p}_2) + g(\vec{p}_1,\vec{p}_2)\vec{\sigma}_1\cdot\vec{\sigma}_2 \\ & + h(\vec{p}_1,\vec{p}_2)S_{12}(\hat{q}) + k(\vec{p}_1,\vec{p}_2)S_{12}(\hat{P}) \\ & + \ell(\vec{p}_1,\vec{p}_2)(\vec{\sigma}_1\times\vec{\sigma}_2)\cdot(\hat{q}\times\hat{P}),\end{aligned} \tag{2}$$

and analogously for $\mathcal{A}'$ with the replacement $\{f,g,h,k,\ell\} \longrightarrow \{f',g',h',k',\ell'\}$. The relative momentum is defined by $\vec{q} = \vec{p}_1 - \vec{p}_2$ and the center of mass momentum is given by $\vec{P} = \vec{p}_1 + \vec{p}_2$. The tensor operator has the usual form $S_{12}(\hat{v}) = 3\vec{\sigma}_1\cdot\hat{v}\,\vec{\sigma}_2\cdot\hat{v} - \vec{\sigma}_1\cdot\vec{\sigma}_2$. The interaction in Eq. (2) is invariant under rotations, time-reversal, parity, and the exchange of particle labels. The presence of the medium breaks Galilean invariance, and two new structures [the "center-of-mass tensor" $S_{12}(\hat{P})$ and "cross-vector" $(\vec{\sigma}_1\times\vec{\sigma}_2)\cdot(\hat{q}\times\hat{P})$ operators] arise [15] that depend explicitly on the center-of-mass momentum $\vec{P}$. Neither of these terms are found in the free-space nucleon-nucleon potential.

By assumption the two quasiparticle momenta $\vec{p}_1$ and $\vec{p}_2$ lie on the Fermi surface ($|\vec{p}_1| = |\vec{p}_2| = k_f$) and therefore the scalar functions $\{f,g,h,k,\ell,f',g',h',k',\ell'\}$ admit a decomposition in Legendre polynomials:

$$\begin{aligned} f(\vec{p}_1,\vec{p}_2) &= \sum_{L=0}^{\infty} f_L(k_f)P_L(\cos\theta), \\ f'(\vec{p}_1,\vec{p}_2) &= \sum_{L=0}^{\infty} f'_L(k_f)P_L(\cos\theta),\ldots \end{aligned} \tag{3}$$

where $\cos\theta = \hat{p}_1\cdot\hat{p}_2$ and $q = 2k_f\sin(\theta/2)$ and $P = 2k_f\cos(\theta/2)$. The expansion coefficients $f_L, f'_L, \ldots$ are referred to as the Fermi liquid parameters. In relating the Fermi liquid parameters to nuclear observables, it is often convenient to multiply by the density of states

$$N_0 = 2M^*k_f/\pi^2, \tag{4}$$

with M^* the effective nucleon mass, to obtain dimensionless parameters $F_L = N_0 f_L, \ldots$.

The ten scalar functions in Eq. (2) can be extracted from linear combinations of the spin-space and isospin-space matrix elements, but the decomposition will depend on the orientation of the orthogonal vectors $\vec{q}$ and $\vec{P}$. For instance, if $\vec{P} = P\hat{z}$ and $\vec{q} = q\hat{x}$, then

$$\begin{aligned} f &= \big(6\mathcal{F}^1_{1,1;1,1} + 3\mathcal{F}^1_{1,0;1,0} + 3\mathcal{F}^1_{0,0;0,0} \\ &\quad + 2\mathcal{F}^0_{1,1;1,1} + \mathcal{F}^0_{1,0;1,0} + \mathcal{F}^0_{0,0;0,0}\big)/16, \\ f' &= \big(2\mathcal{F}^1_{1,1;1,1} + \mathcal{F}^1_{1,0;1,0} + \mathcal{F}^1_{0,0;0,0} \\ &\quad - 2\mathcal{F}^0_{1,1;1,1} - \mathcal{F}^0_{1,0;1,0} - \mathcal{F}^0_{0,0;0,0}\big)/16, \\ g &= \big(6\mathcal{F}^1_{1,1;1,1} + 3\mathcal{F}^1_{1,0;1,0} - 9\mathcal{F}^1_{0,0;0,0} \\ &\quad + 2\mathcal{F}^0_{1,1;1,1} + \mathcal{F}^0_{1,0;1,0} - 3\mathcal{F}^0_{0,0;0,0}\big)/48, \\ g' &= \big(2\mathcal{F}^1_{1,1;1,1} + \mathcal{F}^1_{1,0;1,0} - 3\mathcal{F}^1_{0,0;0,0} \\ &\quad - 2\mathcal{F}^0_{1,1;1,1} - \mathcal{F}^0_{1,0;1,0} + 3\mathcal{F}^0_{0,0;0,0}\big)/48, \\ h &= \big(3\mathcal{F}^1_{1,1;1,-1} + \mathcal{F}^0_{1,1;1,-1}\big)/12, \\ h' &= \big(\mathcal{F}^1_{1,1;1,-1} - \mathcal{F}^0_{1,1;1,-1}\big)/12, \\ k &= \big(3\mathcal{F}^1_{1,1;1,1} - 3\mathcal{F}^1_{1,0;1,0} + 3\mathcal{F}^1_{1,1;1,-1} \\ &\quad + \mathcal{F}^0_{1,1;1,1} - \mathcal{F}^0_{1,0;1,0} + \mathcal{F}^0_{1,1;1,-1}\big)/24, \\ k' &= \big(\mathcal{F}^1_{1,1;1,1} - \mathcal{F}^1_{1,0;1,0} + \mathcal{F}^1_{1,1;1,-1} \\ &\quad - \mathcal{F}^0_{1,1;1,1} + \mathcal{F}^0_{1,0;1,0} - \mathcal{F}^0_{1,1;1,-1}\big)/24, \\ \ell &= \big(3\mathcal{F}^1_{1,1;0,0} + \mathcal{F}^0_{1,1;0,0}\big)/4\sqrt{2}, \\ \ell' &= \big(\mathcal{F}^1_{1,1;0,0} - \mathcal{F}^0_{1,1;0,0}\big)/4\sqrt{2}, \end{aligned} \tag{5}$$

with the notation $\mathcal{F}^T_{S,m_s;S',m'_s} = \langle Sm_sT|\mathcal{F}|S'm'_sT\rangle$.

The quasiparticle interaction is defined as the second functional derivative of the energy E with respect to the occupation

probabilities $n_{\vec{p}st}$:

$$\delta E = \sum_{\vec{p}_1 s_1 t_1} \epsilon_{\vec{p}_1}\, \delta n_{\vec{p}_1 s_1 t_1} + \frac{1}{2\Omega} \sum_{\substack{\vec{p}_1 s_1 t_1 \\ \vec{p}_2 s_2 t_2}} \mathcal{F}(\vec{p}_1 s_1 t_1; \vec{p}_2 s_2 t_2) \delta n_{\vec{p}_1 s_1 t_1} \delta n_{\vec{p}_2 s_2 t_2}, \quad (6)$$

where Ω is a normalization volume. The quasiparticle interaction $\mathcal{F}$ in momentum space has units fm^2, s_i labels the spin quantum number of quasiparticle i, and t_i labels the isospin quantum number. In the present work we consider contributions to the quasiparticle interaction up to second order in many-body perturbation theory.

B. Two-body force contributions

The first- and second-order terms in the perturbative expansion of the ground-state energy from two-body forces are given by

$$E^{(1)}_{2N} = \frac{1}{2} \sum_{ij} n_i n_j \langle ij|\overline{V}_{2N}|ij\rangle, \quad (7)$$

$$E^{(2)}_{2N} = \frac{1}{4} \sum_{ijmn} |\langle ij|\overline{V}_{2N}|mn\rangle|^2 \frac{n_i n_j \bar{n}_m \bar{n}_n}{e_i + e_j - e_m - e_n}, \quad (8)$$

where $n_j = \theta(k_f - |\vec{k}_j|)$, $\bar{n}_j = 1 - n_j = \theta(|\vec{k}_j| - k_f)$, and $\overline{V}$ indicates an antisymmetrized interaction. In Eqs. (7) and (8) the sums run over momentum, spin, and isospin.

Functionally differentiating Eq. (7) with respect to (arbitrary distribution functions) n_1 and n_2 yields for the first-order contribution to the quasiparticle interaction

$$\mathcal{F}^{(1)}_{2N}(\vec{p}_1 s_1 t_1; \vec{p}_2 s_2 t_2) = \langle 12|\overline{V}_{2N}|12\rangle = \langle \vec{p}_1 s_1 t_1; \vec{p}_2 s_2 t_2|\overline{V}_{2N}|\vec{p}_1 s_1 t_1; \vec{p}_2 s_2 t_2\rangle, \quad (9)$$

shown diagrammatically in Fig. 1(a). Since this is just a matrix element of the antisymmetrized free-space nucleon-nucleon potential, only the four central and two exchange-tensor terms in the quasiparticle interaction can be generated and the total spin $\vec{S} = (\vec{\sigma}_1 + \vec{\sigma}_2)/2$ (with associated quantum number S) is conserved. From the second-order energy in Eq. (8), three different contributions to the quasiparticle interaction arise which are distinguished by intermediate particle-particle, hole-hole, and particle-hole states shown diagrammatically in Figs. 1(b)–1(d), respectively. They have the form

$$\mathcal{F}^{(2pp)}_{2N}(\vec{p}_1 s_1 t_1; \vec{p}_2 s_2 t_2) = \frac{1}{2} \sum_{mn} \frac{|\langle 12|\overline{V}_{2N}|mn\rangle|^2 \bar{n}_m \bar{n}_n}{\epsilon_1 + \epsilon_2 - \epsilon_m - \epsilon_n}, \quad (10)$$

$$\mathcal{F}^{(2hh)}_{2N}(\vec{p}_1 s_1 t_1; \vec{p}_2 s_2 t_2) = \frac{1}{2} \sum_{ij} \frac{|\langle ij|\overline{V}_{2N}|12\rangle|^2 n_i n_j}{\epsilon_i + \epsilon_j - \epsilon_1 - \epsilon_2}, \quad (11)$$

$$\mathcal{F}^{(2ph)}_{2N}(\vec{p}_1 s_1 t_1; \vec{p}_2 s_2 t_2) = -2 \sum_{jn} \frac{|\langle 1j|\overline{V}_{2N}|2n\rangle|^2 n_j \bar{n}_n}{\epsilon_1 + \epsilon_j - \epsilon_2 - \epsilon_n}. \quad (12)$$

Equations (9)–(12) can be evaluated for realistic nuclear interactions by first decomposing the potential matrix elements into partial-wave sums. The Fermi liquid parameters are then obtained by integrating over the angle θ between $\vec{p}_1$ and $\vec{p}_2$ with appropriate Legendre polynomials as weighting functions. For the first-order term, as well as the second-order particle-particle and hole-hole diagrams, the partial-wave decomposition is straightforward since the two quasiparticle states are both in the incoming or outgoing state. However, the evaluation of the second-order particle-hole diagram is more complicated due to the cross coupling of the quasiparticle states in one incoming and one outgoing state. We state here the final expressions, and for additional details the reader is referred to Ref. [45]. As already mentioned, the first-order contribution to the quasiparticle interaction is just a matrix element of the antisymmetrized free-space potential:

$$\mathcal{F}^{(1)}_L(Sm_s m'_s; T) = 16\pi(2L+1) \sum_{ll'J} i^{l-l'} \sqrt{(2l+1)(2l'+1)}\, \langle l0\, Sm_s|JM\rangle \times \langle l'0\, Sm'_s|JM\rangle \int_0^{k_f} dp\, \frac{p}{k_f^2}\, \langle plSJT|V_{2N}|pl'SJT\rangle P_L\big(1 - 2p^2/k_f^2\big), \quad (13)$$

where $p = q/2$. The second-order terms are given by

$$\mathcal{F}^{(2pp)}_L(Sm_s m'_s; T) = \frac{16(2L+1)}{k_F^2} \sum_{\substack{l_1 l_2 l_3 l_4 m m' \\ \bar{m}\bar{m}_s J J' M}} \int_0^{k_F} dp\, p P_L\big(1 - 2p^2/k_f^2\big) \int_p^{\infty} dk\, k^2 N(l_1 m l_2 \bar{m} l_3 m' l_4 \bar{m}) P^m_{l_1}(0) P^{m'}_{l_3}(0) \times \frac{M}{p^2 - k^2} i^{l_2 + l_3 - l_1 - l_4} \mathcal{C}^{JM}_{l_1 m S m_s} \mathcal{C}^{JM}_{l_2 \bar{m} S \bar{m}_s} \mathcal{C}^{J'M}_{l_3 m' S m'_s} \mathcal{C}^{J'M}_{l_4 \bar{m} S \bar{m}_s} \int_{\max\{-x_0,-1\}}^{\min\{x_0,1\}} dx\, P^{\bar{m}}_{l_2}(x) P^{\bar{m}}_{l_4}(x) \times \langle pl_1 SJT|V_{2N}|kl_2 SJT\rangle \langle kl_4 SJ'T|V_{2N}|pl_3 SJ'T\rangle, \quad (14)$$

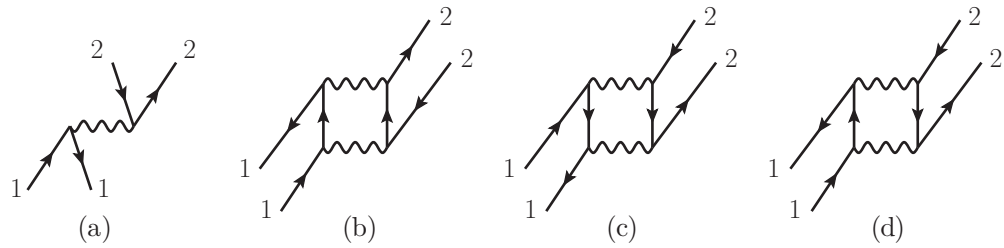

FIG. 1. Diagrams contributing to the quasiparticle interaction (all interactions represented by wavy lines are antisymmetrized): (a) first-order, (b) second-order particle-particle, (c) second-order hole-hole, and (d) second-order particle-hole diagrams.

$$\mathcal{F}_L^{(2hh)}(Sm_sm_s';T)=\frac{16(2L+1)}{k_F^2}\sum_{\substack{l_1l_2l_3l_4mm'\\ \bar{m}\bar{m}_sJJ'M}}\int_0^{k_F}dp\;pP_L\big(1-2p^2/k_f^2\big)\int_0^{p}dk\;k^2N(l_1ml_2\bar{m}l_3m'l_4\bar{m})P_{l_1}^{m}(0)P_{l_3}^{m'}(0)$$
$$\times\frac{M}{k^2-p^2}i^{l_2+l_3-l_1-l_4}\mathcal{C}^{JM}_{l_1mSm_s}\mathcal{C}^{JM}_{l_2\bar{m}S\bar{m}_s}\mathcal{C}^{J'M}_{l_3m'Sm_s'}\mathcal{C}^{J'M}_{l_4\bar{m}S\bar{m}_s}\int_{\max\{x_0,-1\}}^{\min\{-x_0,1\}}dx\;P_{l_2}^{\bar{m}}(x)P_{l_4}^{\bar{m}}(x)$$
$$\times\langle pl_1SJT|V_{2N}|kl_2SJT\rangle\langle kl_4SJ'T|V_{2N}|pl_3SJ'T\rangle, \tag{15}$$

$$\mathcal{F}_L^{(2ph)}(s_1s_2s_1's_2';t_1t_2t_1't_2')=\frac{16(2L+1)}{\pi k_f^2}\int_0^{k_f}dp\;pP_L\big(1-2p^2/k_f^2\big)\int_0^{2\pi}d\phi_3\int_{\max\{0,y_0\}}^{k_f}dk_3k_3^2\int_{\max\{-1,z_0\}}^{1}d\cos\theta_3$$
$$\times\sum_{\substack{l_1l_2l_3l_4s_3s_4\\ m_1m_2m_3m_4}}\langle p'l_1m_1s_1s_3t_1t_3|V|k'l_2m_2s_2s_4t_2t_4\rangle\langle k'l_4m_4s_2's_4t_2't_4|V|p'l_3m_3s_1's_3t_1't_3\rangle$$
$$\times\cos((m_3-m_1+m_2-m_4)\phi_{p'})P_{l_1}^{m_1}(\cos\theta_{p'})P_{l_2}^{m_2}(\cos\theta_{k'})P_{l_3}^{m_3}(\cos\theta_{p'})P_{l_4}^{m_4}(\cos\theta_{k'})$$
$$\times i^{l_2+l_3-l_1-l_4}N(l_1m_1l_2m_2l_3m_3l_4m_4)\frac{M}{p^2+k_3p\cos\theta_3}, \tag{16}$$

where in the particle-particle and hole-hole diagrams $\vec{k}=(\vec{k}_3-\vec{k}_4)/2$, $x_0=(k^2-p^2)/(2k\sqrt{k_f^2-p^2})$, $x=\cos\theta_k$, P_l^m are the associated Legendre functions, and $N(l_1m_1l_2m_2l_3m_3l_4m_4)=N_{l_1}^{m_1}N_{l_2}^{m_2}N_{l_3}^{m_3}N_{l_4}^{m_4}$ with $N_l^m=\sqrt{(2l+1)(l-m)!/(l+m)!}$. In the particle-hole diagram we have additionally $\vec{p}\,'=(\vec{p}_1-\vec{k}_3)/2$, $\vec{k}'=(\vec{p}_2-\vec{k}_4)/2$, $y_0=k_f-2p$, and $z_0=(k_f^2-k_3^2-4p^2)/(4k_3p)$. From the matrix elements of the second-order particle-hole contribution in the uncoupled spin and isospin basis, it is trivial to generate through recoupling the terms needed in Eq. (5) to extract the Fermi liquid parameters.

Given the numerical complexity of Eqs. (14)–(16), we benchmark our codes against semianalytical results from model interactions. As a first case we consider a modified pseudoscalar interaction of the form

$$V_{ps}=g^2\frac{\vec{\sigma}_1\cdot\vec{q}\;\vec{\sigma}_2\cdot\vec{q}}{(m^2+q^2)^2}\vec{\tau}_1\cdot\vec{\tau}_2, \tag{17}$$

where $\vec{q}$ is the momentum transfer, g is a dimensionless coupling constant, and m is the mass parameter chosen to be large enough to achieve good convergence in momentum integrals and partial wave summations. We choose for concreteness $g=6$ and $m=600$ MeV. As a second interesting case, we consider the interference between an isoscalar central and spin-orbit interaction of the form

$$V_c=g^2\frac{1}{m^2+q^2}, \tag{18}$$

$$V_{so}=\frac{g^2}{m^2}\frac{i\,(\vec{\sigma}_1+\vec{\sigma}_2)\cdot(\vec{q}\times\vec{p}\,)}{m^2+q^2}, \tag{19}$$

where $\vec{p}$ is the incoming relative momentum. We choose the same values for g and m as in the modified pseudoscalar case above.

In Ref. [45] it was shown that the second-order particle-particle and hole-hole diagrams can only generate the central, relative momentum tensor, and center-of-mass tensor components of the quasiparticle interaction. In fact, only the combination of a spin-orbit force with any non-spin-orbit force in the second-order particle-hole diagram can lead to a cross-vector term. These general conclusions are exemplified for the test interactions considered in Eqs. (17)–(19). In particular, the $L=0,1$ isoscalar relative-momentum tensor and center-of-mass tensor Fermi liquid parameters from modified pseudoscalar exchange at second order are shown in the left and middle plots of Fig. 2 employing both the partial-wave decomposition in Eqs. (14)–(16) as well as semianalytical expressions similar to those in Sec. III of Ref. [45]. The isovector contributions only differ from the isoscalar contributions by integer factors

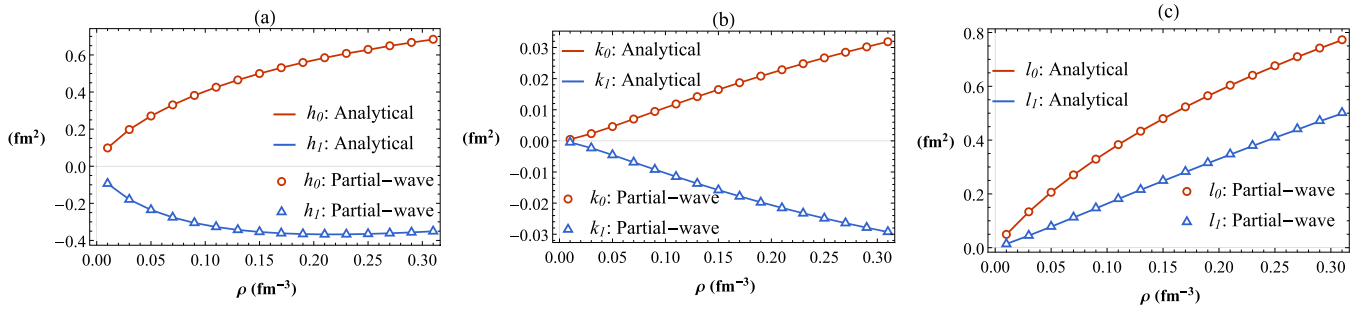

FIG. 2. Comparison of the $L = 0,1$ noncentral Fermi liquid parameters in nuclear matter from modified pseudoscalar exchange at second order (left and middle plots) as well as from the interference of a central and spin-orbit interaction in the particle-hole channel (right plot). Results from both a partial-wave decomposition and semianalytical calculation are compared and found to be in excellent agreement.

and therefore are not shown explicitly. The modified pseudoscalar interaction at second order also gives rise to central components of the quasiparticle interaction, but these have been considered in a previous work [64]. From Fig. 2 we see that the numerical agreement across the full range of densities considered, $0 < \rho < 0.32$ fm^{-3}, is excellent. In the rightmost plot of Fig. 2 we show the Fermi liquid parameters associated with the cross-vector interaction from the interference term between a central and spin-orbit force. Again the numerical agreement between the two methods is very good.

C. Three-body force contributions

We next consider contributions to the quasiparticle interaction from three-body forces. The Hartree-Fock energy is given by

$$E_{3N}^{(1)} = \frac{1}{6}\sum_{ijk} n_i n_j n_k \langle ijk|\overline{V}_{3N}|ijk\rangle, \tag{20}$$

where the totally antisymmetrized three-body potential is defined by $\overline{V}_{3N} = (1 - P_{12} - P_{13} - P_{23} + P_{12}P_{23} + P_{12}P_{13})V_{3N}$. In the present work we employ the N2LO chiral three-body force, which includes a long-range two-pion exchange component $V_{3N}^{2\pi}$, a one-pion exchange contribution $V_{3N}^{1\pi}$, and a pure contact force $V_{3N}^{\rm cont}$. The two-pion exchange three-nucleon interaction has the form

$$V_{3N}^{2\pi} = \sum_{i\neq j\neq k} \frac{g_A^2}{8f_\pi^4} \frac{\vec{\sigma}_i\cdot\vec{q}_i\,\vec{\sigma}_j\cdot\vec{q}_j}{(\vec{q}_i^{\,2}+m_\pi^2)(\vec{q}_j^{\,2}+m_\pi^2)} F_{ijk}^{\alpha\beta}\tau_i^\alpha\tau_j^\beta, \tag{21}$$

where $g_A = 1.29$, $f_\pi = 92.2$ MeV, $m_\pi = 138$ MeV denotes the average pion mass, $\vec{q}_i$ denotes the difference between the final and initial momenta of nucleon i, and the isospin tensor $F_{ijk}^{\alpha\beta}$ is given by

$$F_{ijk}^{\alpha\beta} = \delta^{\alpha\beta}\left(-4c_1m_\pi^2 + 2c_3\vec{q}_i\cdot\vec{q}_j\right) + c_4\epsilon^{\alpha\beta\gamma}\tau_k^\gamma\vec{\sigma}_k\cdot(\vec{q}_i\times\vec{q}_j). \tag{22}$$

The one-pion exchange component of the three-nucleon interaction reads

$$V_{3N}^{1\pi} = -\sum_{i\neq j\neq k} \frac{g_A c_D}{8f_\pi^4\Lambda_\chi} \frac{\vec{\sigma}_j\cdot\vec{q}_j}{\vec{q}_j^{\,2}+m_\pi^2}\vec{\sigma}_i\cdot\vec{q}_j\,\vec{\tau}_i\cdot\vec{\tau}_j, \tag{23}$$

where $\Lambda_\chi = 700$ MeV. Finally, the three-nucleon contact interaction has the form

$$V_{3N}^{\rm cont} = \sum_{i\neq j\neq k} \frac{c_E}{2f_\pi^4\Lambda_\chi}\vec{\tau}_i\cdot\vec{\tau}_j. \tag{24}$$

In pure neutron matter only the terms proportional to c_1 and c_3 contribute to the ground state energy and quasiparticle interaction, but for symmetric nuclear matter in general all terms are needed. Taking two functional derivatives of Eq. (20) with respect to n_1 and n_2 yields

$$\mathcal{F}_{3N}^{(1)}(\vec{p}_1s_1t_1,\vec{p}_2s_2t_2) = \frac{1}{3}\sum_i n_i[\langle i12|\overline{V}_{3N}|i12\rangle + \langle 1i2|\overline{V}_{3N}|1i2\rangle + \langle 12i|\overline{V}_{3N}|12i\rangle]. \tag{25}$$

Since the three-body force is symmetric under the interchange of particle labels, we can rewrite Eq. (25) without loss of generality as

$$\mathcal{F}_{3N}^{(1)}(\vec{p}_1s_1t_1,\vec{p}_2s_2t_2) = \sum_i n_i\langle i12|\overline{V}_{3N}|i12\rangle. \tag{26}$$

In general there are nine distinct direct (and exchange) contributions to the quasiparticle interaction from a three-body force. In Fig. 3 we show the direct terms from the N2LO chiral three-nucleon interaction (exchange terms can be obtained by swapping the two outgoing lines). As seen in Fig. 3 there are three topologically distinct contributions from the two-pion exchange three-body force $V_{3N}^{2\pi}$. Contribution "(2)" represents the sum of four reflected diagrams, while contribution "(3)" represents the sum of two reflected diagrams. The one-pion exchange contribution $V_{3N}^{1\pi}$ gives rise to two topologically distinct diagrams, shown as "(4)" and "(5)" in Fig. 3. Finally, there is a single diagram "(6)" coming from the three-body contact force $V_{3N}^{\rm cont}$. As shown in the Appendix, this diagram contributes only to the central components of the quasiparticle interaction.

At second order in perturbation theory we include the effects of three-body forces by first constructing a density-dependent two-body force $V_{2N}^{\rm med}$, as described in detail in Refs. [65,66]. In Eqs. (10)–(12) we then replace $\overline{V}_{2N}$ with $\overline{V}_{2N}^{\rm eff} = \overline{V}_{2N} + \overline{V}_{2N}^{\rm med}$. This approximation accounts for only a subset of the full second-order contributions from three-body forces.

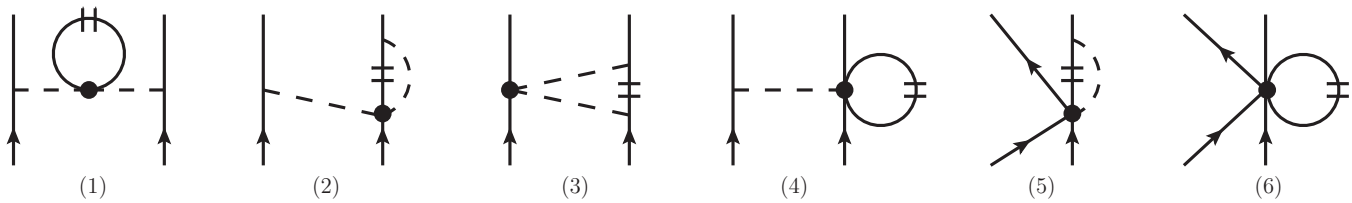

FIG. 3. Diagrammatic contributions to the quasiparticle interaction in symmetric nuclear matter generated from the three terms in the N2LO chiral three-body force. The short double-line symbolizes summation over the filled Fermi sea of nucleons. Reflected diagrams of (2) and (3) are not shown.

III. RESULTS

In the present section we focus on the noncentral components of the quasiparticle interaction from the five different chiral nuclear forces {n2lo450, n2lo500, n3lo414, n3lo450, n3lo500} [46–51]. We focus primarily on the role of three-body forces and second-order perturbative contributions. The quality of the nuclear force models and perturbative many-body method is benchmarked by comparing the nuclear incompressibility, isospin asymmetry energy, and effective mass (which are related to specific central Fermi liquid parameters) with empirical values. We also study the convergence of the expansion of the quasiparticle interaction in Legendre polynomials for both central and noncentral forces.

A. First-order perturbative contributions to Fermi liquid parameters

At first order in perturbation theory, two-nucleon forces contribute only to the relative momentum tensor noncentral Fermi liquid parameters (H_L, H_L') due to the underlying Galilean invariance of the free-space interaction. In Fig. 4 we show as solid-circle and solid-square symbols the magnitude of the dimensionless Fermi liquid parameters (H_0, H_1) and (H_0', H_1') from two-body forces as a function of density. The error bars are calculated as the standard deviation of the results from the five nucleon-nucleon potentials considered in the present work and represent an estimate of systematic uncertainties in the construction of realistic two- and three-body force models. Note that here and in the following sections, we employ in the density of states, Eq. (4), the Landau effective mass computed from the full quasiparticle interaction including second-order perturbative contributions [see Eq. (42) below]. The Hartree-Fock single-particle spectrum is used only when calculating the energy denominators in the second-order perturbative contributions to the quasiparticle interaction. Comparing the results from two-body forces in Fig. 4, we find the approximate relationship $H_0 \simeq -3H_0'$ and $H_1 \simeq -3H_1'$, which in fact exactly holds for all L in the case of a pure one-pion exchange (OPE) nucleon-nucleon potential [39].

Next we present analytical expressions for the noncentral Fermi liquid parameters in nuclear matter from the N2LO chiral three-nucleon interaction. The associated low-energy constants $\{c_1, c_3, c_4, c_D, c_E\}$ have been fitted separately for each nuclear potential and are compiled in Table I.

We present individually the Fermi liquid parameters arising from the five diagrammatic contributions in Fig. 3. The pion self-energy correction $V_{NN}^{\mathrm{med},1}$ leads to a relative-momentum tensor interaction

$$h_L = -3h_L' = \frac{g_A^2 m_\pi^3 u^5}{3\pi^2 f_\pi^4} \int_{-1}^{1} dz\,(1-z)(2L+1) \times P_L(z)\,\frac{c_3 u^2(z-1)-c_1}{[1+2u^2(1-z)]^2}, \tag{27}$$

where $u = k_f/m_\pi$ and $P_L(z)$ is the Legendre polynomial of degree L. The pion-exchange vertex correction, $V_{NN}^{\mathrm{med},2}$, likewise gives rise to relative-tensor force of the form

$$\begin{aligned} h_L = -3h_L' = {} & \frac{g_A^2 m_\pi^3}{\pi^2 (4f_\pi)^4} \int_{-1}^{1} dz\,\frac{(1-z)(2L+1)P_L(z)}{1+2u^2(1-z)} \\ & \times \left\{ \frac{64u^2}{3}(c_3-2c_4)\arctan 2u + \left[\frac{(c_3+c_4)\left(\frac{1}{3}-z\right)-4c_1}{u} \right.\right. \\ & \left. + 4u(3c_4-4c_1-c_3-(c_3+c_4)z) + \right] \ln(1+4u^2) \\ & + 4(c_3+c_4)uz\left(1+2u^2-\frac{8u^4}{3}\right) + \frac{32u^5}{9}(5c_3-7c_4) \\ & \left. + 8u^3(4c_1-3c_3+5c_4) + \frac{4u}{3}(12c_1-c_3-c_4) \right\}. \end{aligned} \tag{28}$$

Since $V_{NN}^{\mathrm{med},1}$ and $V_{NN}^{\mathrm{med},2}$ renormalize the one-pion exchange interaction through self-energy and vertex corrections, the associated Fermi liquid parameters obey the generic relationship $h_L = -3h_L'$ as seen explicitly above.

The Pauli-blocked two-pion exchange contribution, $V_{NN}^{\mathrm{med},3}$, gives rise to a richer set of spin and isospin structures that lead to contributions to all of the noncentral Fermi liquid parameters

TABLE I. Low-energy constants associated with the N2LO chiral three-body force for the five different nuclear potentials considered in the present work. The constants c_1, c_3, and c_4 have units GeV^{-1}, while c_D and c_E are unitless.

	c_1	c_3	c_4	c_D	c_E
n2lo450	−0.81	−3.40	3.40	−0.326	−0.149
n2lo500	−0.81	−3.40	3.40	−0.165	−0.169
n3lo414	−0.81	−3.00	3.40	−0.400	−0.072
n3lo450	−0.81	−3.40	3.40	−0.240	−0.106
n3lo500	−0.81	−3.20	5.40	−0.200	−0.205

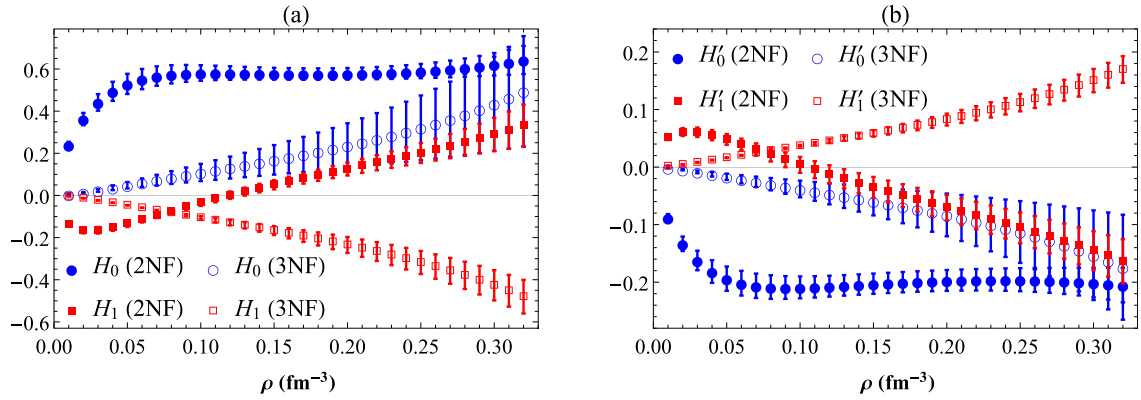

FIG. 4. First-order perturbative contributions to the dimensionless $L = 0,1$ Fermi liquid parameters of the relative tensor interactions as a function of density. Results for both two- and three-body forces are included.

(h,h',k,k',ℓ,ℓ'). For the relative tensor interaction we find

$$\begin{aligned} h_L &= -3h'_L \\ &= \frac{g_A^2 c_4 m_\pi^3 u^2}{16\pi^3 f_\pi^4} \int_0^u dl\, l^2 \int_{-1}^1 dx \int_{-1}^1 dy \int_0^\pi d\phi\, (2L+1) P_L(z) \frac{(1-z)[u(1+z)-l(x+y)]^2}{(1+z)(1+u^2+l^2-2ulx)(1+u^2+l^2-2uly)}, \end{aligned} \tag{29}$$

with $z = xy + \sqrt{(1-x^2)(1-y^2)}\cos\phi$. The center-of-mass tensor Fermi liquid parameters in the isoscalar and isovector channel are given by

$$\begin{aligned} k_L = -3k'_L = \frac{g_A^2 c_4 m_\pi^3 u^2}{16\pi^3 f_\pi^4} &\int_0^u dl\, l^2 \int_{-1}^1 dx \int_{-1}^1 dy \int_0^\pi d\phi\, (2L+1) P_L(z) \\ &\times \frac{(1-z)[u(1+z)-l(x+y)]^2 + 2l^2(x^2+y^2+z^2-1-2xyz)}{(1+z)(1+u^2+l^2-2ulx)(1+u^2+l^2-2uly)}. \end{aligned} \tag{30}$$

We note that the relative tensor interaction exhibits the same relationship, $k_L = -3k'_L$, between the isoscalar and isovector components as the relative-momentum tensor interactions above. Finally, the Pauli-blocked two-pion exchange diagram produces a cross-vector interaction with Fermi liquid parameters,

$$\begin{aligned} \ell_L &= \frac{3g_A^2 m_\pi^3 u}{32\pi^3 f_\pi^4} \int_0^u dl\, l^2 \int_{-1}^1 dx \int_{-1}^1 dy \int_0^\pi d\phi\, (2L+1) P_L(z) \sqrt{\frac{1-z}{1+z}} \\ &\quad \times [u(1+z)-l(x+y)] \frac{2c_1 + (c_3-c_4)[l^2 - ul(x+y) + u^2 z]}{(1+u^2+l^2-2ulx)(1+u^2+l^2-2uly)}, \end{aligned} \tag{31}$$

$$\begin{aligned} \ell'_L &= \frac{g_A^2 m_\pi^3 u}{32\pi^3 f_\pi^4} \int_0^u dl\, l^2 \int_{-1}^1 dx \int_{-1}^1 dy \int_0^\pi d\phi\, (2L+1) P_L(z) \sqrt{\frac{1-z}{1+z}} \\ &\quad \times [u(1+z)-l(x+y)] \frac{6c_1 + (3c_3+c_4)[l^2 - ul(x+y) + u^2 z]}{(1+u^2+l^2-2ulx)(1+u^2+l^2-2uly)}, \end{aligned} \tag{32}$$

$$\begin{aligned} \tilde{\ell}_L &= \frac{3g_A^2 m_\pi^3 u}{16\pi^3 f_\pi^4} \int_0^u dl\, l^2 \int_{-1}^1 dx \int_{-1}^1 dy \int_0^\pi d\phi\, (2L+1) P_L(z) \\ &\quad \times [u(1+z)-l(x+y)] \frac{2c_1 + (c_3-c_4)[l^2 - ul(x+y) + u^2 z]}{(1+u^2+l^2-2ulx)(1+u^2+l^2-2uly)}, \end{aligned} \tag{33}$$

$$\begin{aligned} \tilde{\ell}'_L &= \frac{g_A^2 m_\pi^3 u}{16\pi^3 f_\pi^4} \int_0^u dl\, l^2 \int_{-1}^1 dx \int_{-1}^1 dy \int_0^\pi d\phi\, (2L+1) P_L(z) \\ &\quad \times [u(1+z)-l(x+y)] \frac{6c_1 + (3c_3+c_4)[l^2 - ul(x+y) + u^2 z]}{(1+u^2+l^2-2ulx)(1+u^2+l^2-2uly)}. \end{aligned} \tag{34}$$

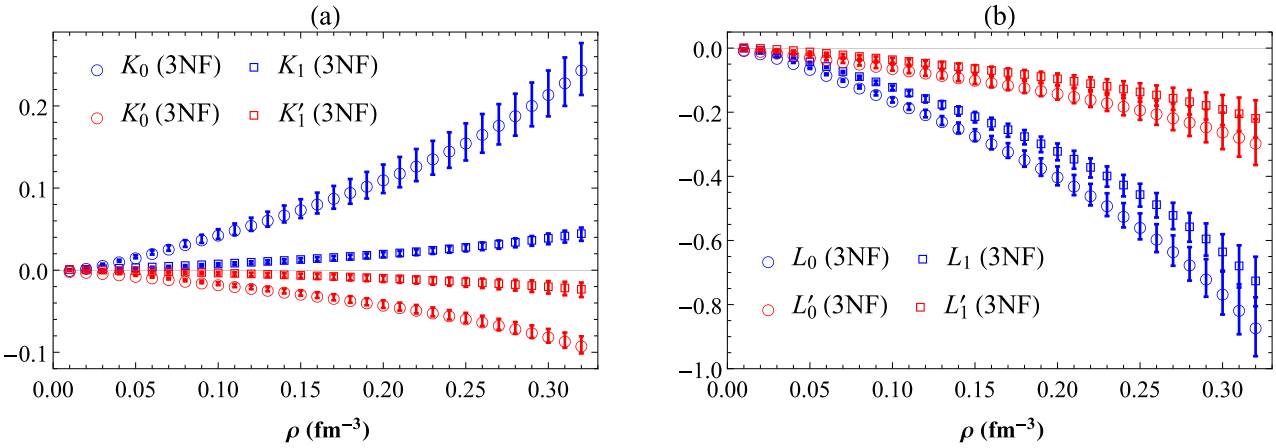

FIG. 5. First-order perturbative contributions to the dimensionless $L = 0,1$ Fermi liquid parameters of the center-of-mass tensor and cross-vector interactions as a function of density. Only three-body forces contribute at the Hartree-Fock level.

In Eqs. (31)–(34) we have employed two versions of the cross-vector quasiparticle interaction in terms of Fermi liquid parameters:

$$\mathcal{F}_{\rm cross} = (\vec{\sigma}_1 \times \vec{\sigma}_2) \cdot (\hat{q} \times \hat{P}) \sum_{L=0}^{\infty} \ell_L(k_f)\, P_L(\hat{p}_1 \cdot \hat{p}_2), \quad (35)$$

and

$$\mathcal{F}_{\rm cross} = \frac{(\vec{\sigma}_1 \times \vec{\sigma}_2) \cdot (\vec{p}_1 \times \vec{p}_2)}{|\vec{p}_1 + \vec{p}_2|^2} \sum_{L=0}^{\infty} \tilde{\ell}_L(k_f)\, P_L(\hat{p}_1 \cdot \hat{p}_2), \quad (36)$$

the latter being more convenient in calculations of nuclear response functions [19]. In pure neutron matter $V_{NN}^{\rm med,3}$ gives rise to only central and cross-vector interactions [45]. In the present symmetric nuclear matter calculation also the relative tensor and center-of-mass tensor terms are generated due to the three-body force proportional to the low-energy constant c_4.

The medium-dependent vertex correction, $V_{NN}^{\rm med,4}$, from the one-pion exchange three-body force leads to a relative tensor force with associated Fermi liquid parameters

$$h_L = -3h_L' = \frac{g_A c_D m_\pi^3 u^5}{24\pi^2 f_\pi^4 \Lambda_\chi} \int_{-1}^{1} dz\, \frac{(1-z)(2L+1)P_L(z)}{1+2u^2(1-z)}. \quad (37)$$

The second contribution, $V_{NN}^{\rm med,5}$, from the one-pion exchange three-body force has the form of a zero-range interaction with vertex correction, leading to a finite-range force that contributes to only the $L = 0,1$ Fermi liquid parameters:

$$h_0 = -h_0' = -h_1 = h_1' = k_0 = -k_0' = k_1 = -k_1' \quad (38)$$
$$= \frac{g_A c_D m_\pi^3}{\pi^2 (4 f_\pi)^4 \Lambda_\chi} \left\{ \frac{1}{u} + 2u - \frac{8u^3}{3} - \frac{1+4u^2}{4u^3} \ln(1+4u^2) \right\}.$$

Finally, the contribution $V_{NN}^{\rm med,6}$ due to the three-body contact interaction is momentum-independent and therefore does not give rise to any noncentral components of the quasiparticle interaction.

In Figs. 4 and 5 we show as open symbols the $L = 0,1$ Fermi liquid parameters associated with the N2LO chiral three-body force as a function of density computed at the Hartree-Fock level according to Eq. (26). All contributions vanish in the $\rho \to 0$ limit and grow approximately linearly with the density up to nuclear saturation density $\rho_0 = 0.16$ fm^{-3}. We find that in the case of the isotropic H_0 and H_0' Fermi liquid parameters, the three-body force enhances the contribution from two-body forces at all densities considered. In contrast, both H_1 and H_1' from two- and three-body forces exhibit large cancellations beyond nuclear saturation density ρ_0. All three-body force contributions (except $V_{NN}^{\rm med,5}$, which is small) to the relative tensor Fermi liquid parameters obey the relationship $H_L = -3H_L'$ characteristic of one-pion exchange. At the Hartree-Fock level with two- and three-body forces, this relationship turns out to be an excellent approximation relating the isoscalar and isovector relative tensor interactions. The center-of-mass tensor interaction from three-body forces is comparatively weak. The $L = 0,1$ Fermi liquid parameters associated with both the isoscalar and isovector center-of-mass tensor force are all less than 0.10 in magnitude at nuclear matter saturation density. We observe that the spin-nonconserving cross-vector interaction from the chiral three-body force is particularly strong in the isoscalar channel, with L_0 and L_1 from three-body forces reaching values around -0.75 at twice saturation density.

B. Second-order perturbative contributions to Fermi liquid parameters

We next consider the sum of the second-order particle-particle, particle-hole, and hole-hole contributions to the noncentral Fermi liquid parameters. All are computed according to Eqs. (14)−(16), except that a Hartree-Fock energy spectrum for the intermediate particle and hole states is employed. This results in a reduction of the second-order contributions by a density-dependent effective mass factor, which at saturation density is on the order $M_{HF}^*/M \simeq 0.7$. Second-order perturbative contributions [62] to the nucleon self-energy result in a slightly larger average effective mass on the order of $M^*/M \simeq 0.85$ at nuclear saturation density. In the present study we neglect such effects since the associated uncertainties are small compared to the choice of nuclear force model.

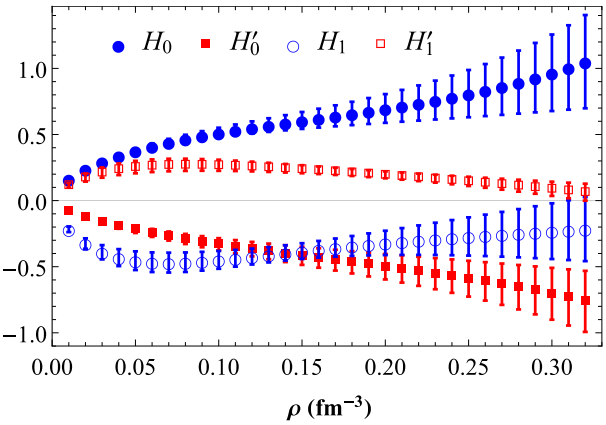

FIG. 6. Total $L = 0,1$ Fermi liquid parameters of the relative tensor interaction from two- and three-body forces as a function of the density. Error bars are obtained from the standard deviation of the five chiral potentials considered in the present work.

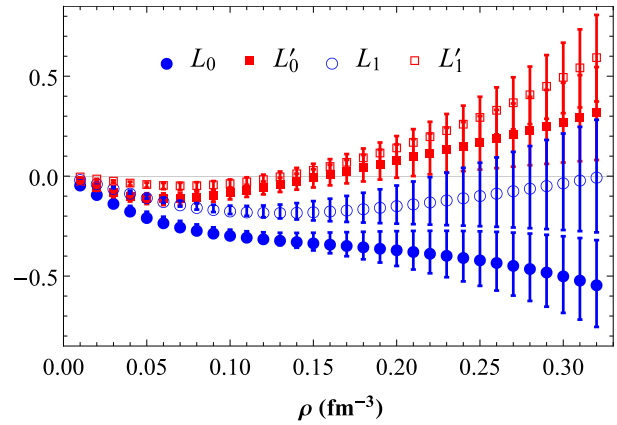

FIG. 8. Total $L = 0,1$ Fermi liquid parameters of the cross-vector interaction from two- and three-body forces as a function of the density. Error bars are obtained from the standard deviation of the five chiral potentials considered in the present work.

In Figs. 6–8 we show the total dimensionless $L = 0,1$ Fermi liquid parameters for the noncentral parts of the quasiparticle interaction as a function of density. This includes the first-order two-body and three-body contributions together with the second-order particle-particle, hole-hole, and particle-hole diagrams. Comparing the results to Figs. 4 and 5, we see that overall the second-order terms have a relatively small impact, in contrast to their large contributions to the central components [44]. Neither the particle-particle nor hole-hole diagram gives any contribution to the noncentral Fermi liquid parameters larger than 0.1 in magnitude across the range of densities considered. The particle-hole diagram, however, gives contributions to the relative tensor and cross-vector Fermi liquid parameters on the order of 0.1–0.3 in magnitude. None of the second-order diagrams lead to a sizable center-of-mass tensor interaction, and in Fig. 7 we see that this component of the quasiparticle interaction is very weak in both the isoscalar and isovector channels in symmetric nuclear matter up to twice saturation density.

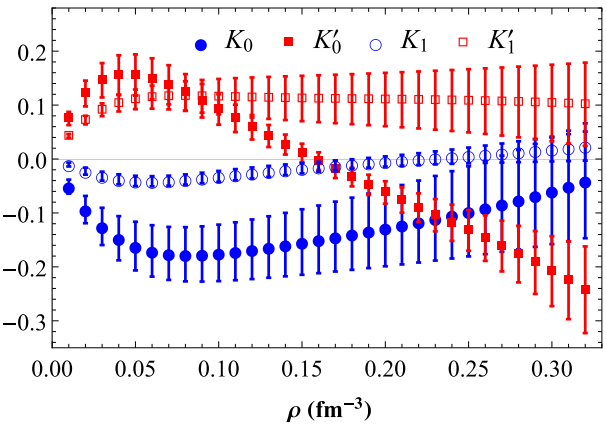

FIG. 7. Total $L = 0,1$ Fermi liquid parameters of the center-of-mass tensor interaction from two- and three-body forces as a function of the density. Error bars are obtained from the standard deviation of the five chiral potentials considered in the present work.

The $L = 0,1$ Fermi liquid parameters of the isoscalar and isovector relative tensor force are very well constrained up to nuclear saturation density. In fact, the uncertainties on all four parameters are less than 0.1 in this regime but grow significantly beyond saturation density. As in the case of one-pion exchange (OPE), the isotropic Landau parameters H_0 and H_0' are respectively positive and negative across all densities considered. The generic relationship $H_L = -3H_L'$, which is satisfied by OPE and most 3NF contributions, is violated due to second-order perturbative contributions. The corresponding tensor interactions in the proton-neutron and proton-proton (neutron-neutron) channels are given by

$$H_L^{pn} = H_L - H_L',$$
$$H_L^{pp} = H_L^{nn} = H_L + H_L'. \tag{39}$$

From Fig. 6 we see that the combination of isoscalar and isovector tensor forces produces a large proton-neutron effective interaction and a very small proton-proton (neutron-neutron) interaction, in agreement with a wide range of experimental data [38].

The Fermi liquid parameters of the cross-vector interaction are non-negligible in the isoscalar channel. In particular, the value of L_0 (and to a lesser extent L_1) grows strongly with the density as a result of the N2LO chiral three-body force. The isovector cross-vector interaction, in contrast, remains small up to about twice saturation density. The large negative value of L_0 may be a concern in light of the normal stability conditions

$$\mathcal{C}_L > -(2L+1), \tag{40}$$

where $\mathcal{C} \in \{F, F', G, G'\}$, for the central components of the quasiparticle interaction. The presence of additional spin-dependent interactions H, K, L (and H', K', L') that couple to G (and G') modifies the stability criteria in Eq. (40), but to date only the effect of the relative tensor contributions have been considered [67].

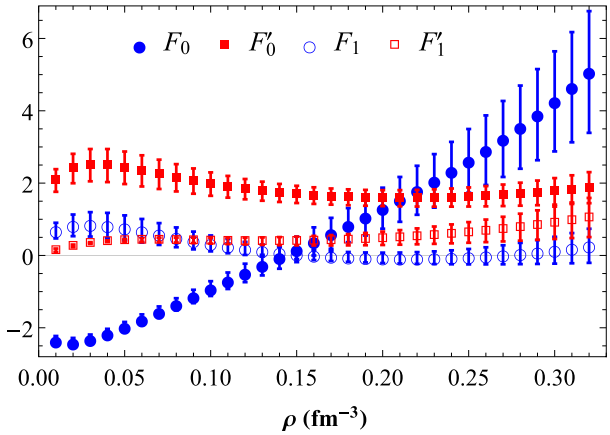

FIG. 9. Total $L = 0,1$ Fermi liquid parameters of the spin-independent central parts of the quasiparticle interaction from two- and three-body forces as a function of the density. Error bars are obtained from the standard deviation of the five chiral potentials considered in the present work.

C. Central components of the quasiparticle interaction

In previous work [44] we have computed the central Fermi liquid parameters in symmetric nuclear matter including the effects of three-body forces. We update those results to include theoretical uncertainties obtained by varying the chiral order and momentum-space cutoff of the nuclear potential. In comparison to Ref. [44] we also consider a larger range of densities in the present calculation. We then use standard relations [68,69] to study various nuclear observables that are directly related to the low-harmonic central Fermi liquid parameters. Since the tensor Fermi liquid parameters for symmetric nuclear matter are largely unconstrained by empirical data, benchmarking the central terms to empirical data is an important check on the nuclear force models and many-body methods.

In Figs. 9 and 10 we show the $L = 0,1$ Fermi liquid parameters associated with the F, F', G, G' components of

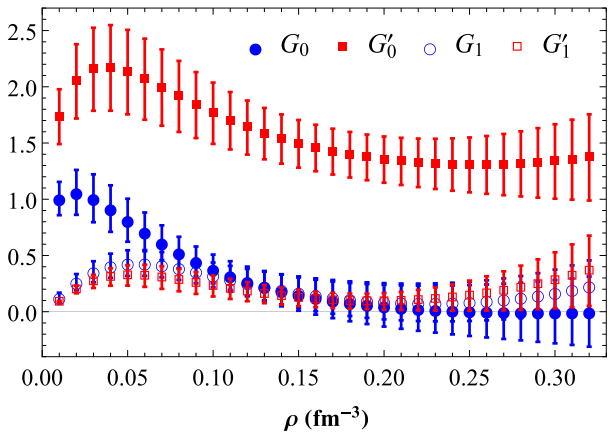

FIG. 10. Total $L = 0,1$ Fermi liquid parameters of the spin-dependent central parts of the quasiparticle interaction from two- and three-body forces as a function of the density. Error bars are obtained from the standard deviation of the five chiral potentials considered in the present work.

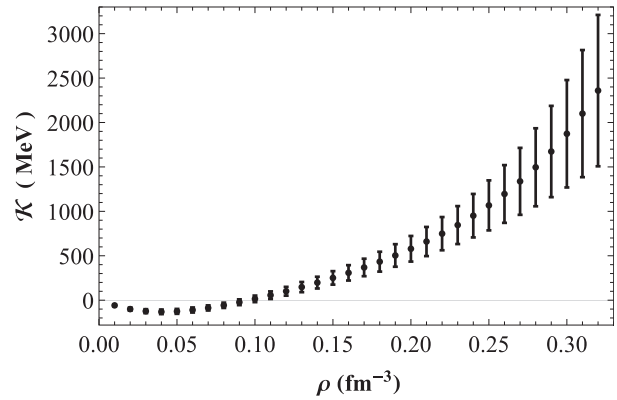

FIG. 11. Incompressibility of symmetric nuclear matter as a function of the density for the two- and three-body chiral nuclear force models considered in the present work.

the quasiparticle interaction. The isotropic spin- and isospin-independent Fermi liquid parameter F_0 is related to the nuclear incompressibility $\mathcal{K} = 9\partial P/\partial\rho$, where $P = \rho^2 \frac{\partial(E/A)}{\partial\rho}$, through

$$\mathcal{K} = \frac{3k_F^2}{M^*}(1 + F_0). \tag{41}$$

From Fig. 9 we see that $F_0 < -1$ for $\rho \lesssim 0.10$ fm^{-3}, which corresponds to the well known instability of nuclear matter to density fluctuations associated with spinodal decomposition and cluster formation. However, the nearly linear dependence of F_0 on the nuclear density results in a strongly increasing nuclear incompressibility, which we show in Fig. 11. At $\rho = \rho_0$ the incompressibility lies in the range 190 MeV $< \mathcal{K} <$ 400 MeV. While this is consistent with the empirical estimate of 220 MeV $< \mathcal{K} <$ 260 MeV [70,71], the large theoretical range is due to the fact the n2lo450, n2lo500, and n3lo500 nuclear forces saturate at too low of a density $\rho \simeq 0.14$–0.15 fm^{-3}. In this case the contribution $18\rho\frac{\partial(E/A)}{\partial\rho}$ beyond saturation density that is linear in the density strongly enhances the nuclear incompressibility.

In Eq. (44) the quasiparticle effective mass M^* is related to the Landau parameter F_1 through

$$\frac{M^*}{M} = 1 + \frac{F_1}{3}, \tag{42}$$

with $M = 938.9182$ MeV the average nucleon mass. From Fig. 9 we find that $F_1 > 0$ for $\rho \lesssim \rho_0$ and consequently the effective mass is larger than the free-space mass. For $\rho \gtrsim \rho_0$ the effective mass may be less than that of a free nucleon, but the decrease in the effective mass with increasing density is not nearly as large as in most mean field models and other approaches to scaling masses [10] at first order. The large effective mass is due almost solely to the second-order particle-hole diagram, which gives a contribution $F_1^{(2ph)} \simeq 1$ for all densities up to $\rho = 2\rho_0$. From the study of nuclear level densities in the vicinity of the Fermi surface, the effective mass has been estimated [72,73] to lie close to that of a free nucleon $M^* \simeq M$. In Fig. 12 we show the effective mass as a function of density together with the theoretical uncertainty estimates. At saturation density we find the range $0.94 < M^*/M < 1.07$.

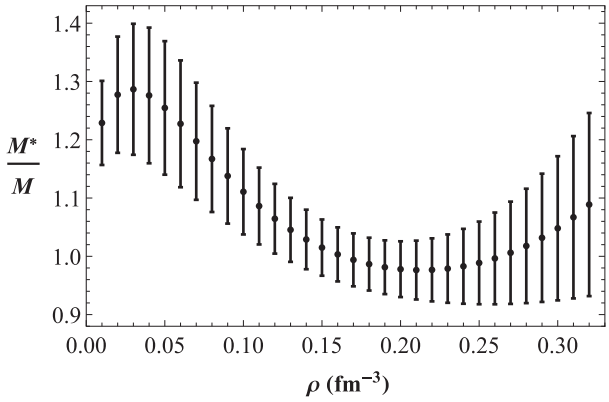

FIG. 12. Nucleon effective mass in symmetric nuclear matter as a function of the density for the two- and three-body chiral nuclear force models considered in the present work.

Since $M^*/M \to 1$ as $\rho \to 0$, the effective mass must rise rather quickly at low densities.

We define the density-dependent isospin-asymmetry energy $S_2(\rho)$ as the coefficient of the quadratic term in an expansion of the energy per particle of isospin-asymmetric nuclear matter in powers of the parameter $\delta_{np} = \frac{\rho_n - \rho_p}{\rho_n + \rho_p}$:

$$\frac{E}{A}(\rho,\delta_{np}) = \frac{E}{A}(\rho,0) + S_2(\rho)\delta_{np}^2 + \cdots . \tag{43}$$

Generically [74,75] the energy per particle contains nonanalytic contributions in δ_{np} beyond the quadratic term in Eq. (43) when second-order perturbative corrections are included in the equation of state, but at low temperatures it is nevertheless a good approximation to retain only the quadratic term in the expansion in Eq. (43). The isospin-asymmetry energy is related to the isotropic part of the F' contribution to the quasiparticle interaction:

$$S_2 = \frac{k_F^2}{6M^*}(1 + F_0'). \tag{44}$$

In Fig. 13 we plot $S_2(\rho)$ and associated uncertainties up to twice nuclear matter saturation density. We find the peculiar

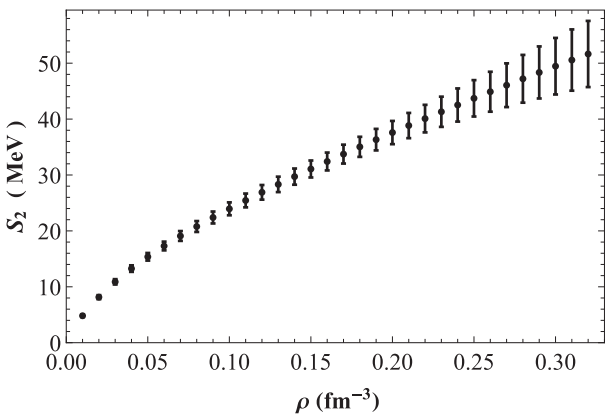

FIG. 13. Isospin-asymmetry energy as a function of the density for the two- and three-body chiral nuclear force models considered in the present work.

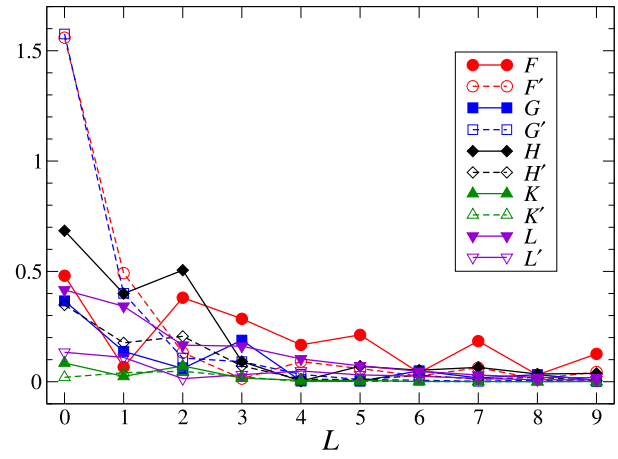

FIG. 14. Convergence of the Legendre polynomial expansion for each of the different contributions to the quasiparticle interaction. Results are shown only for n3lo450 two- and three-body forces at nuclear matter saturation density. Terms up to $L = 9$ are considered.

feature that the variations in the Landau parameter F_1 (which enters into the definition of the effective mass M^*) and in the Landau parameter F_0' are correlated in such a way as to produce a very small error band for the isospin-asymmetry energy up to nuclear saturation density. For instance, at nuclear matter saturation density, we obtain $29.6\ \text{MeV} < S_2(\rho_0) < 33.4\ \text{MeV}$, which is consistent with other recent microscopic uncertainty estimates [59,60] but with a much smaller error band. It is not clear what could lead to the correlation between F_1 and F_0', and therefore we tentatively attribute the very small errors in $S_2(\rho)$ to a chance cancellation.

From Fig. 10 we see that G_0' remains large and positive for all densities considered. At nuclear saturation density, we find $1.16 < G_0' < 1.74$, which is consistent with extractions [76,77] from fitting the peak energy of giant Gamow-Teller resonances in heavy nuclei. Such fits give a range $1.4 < G_0' < 1.6$ [78] but rely on certain model assumptions related to the shape of the parametrized single-particle potential and the form of the effective interaction. In addition the authors of Ref. [78] find correlations between the value of G_1' and the position of the energy peak of the Gamow-Teller resonance when G_0' is kept fixed, leading to further uncertainties in the extraction of G_0' from resonance data.

Finally, we investigate the convergence of the Legendre polynomial decomposition, Eq. (3), for the noncentral components of the quasiparticle interaction. From Figs. 6–8 we see that in some cases the $L = 1$ Fermi liquid parameters are comparable in magnitude to the $L = 0$ parameters at nuclear matter saturation density. Using the tensor parametrizations in Eq. (2), it is expected [16] that the convergence is much improved compared to alternative choices, such as

$$H(\vec{p}_1,\vec{p}_2)S_{12}(\hat{q}) = \frac{q^2}{k_f^2}\tilde{H}(\vec{p}_1,\vec{p}_2)S_{12}(\hat{q}) \tag{45}$$

employed in Refs. [7,14,39]. In Fig. 14 we plot the ten lowest dimensionless Fermi liquid parameters from the n3lo450 potential at nuclear matter saturation density. It is clear that

the slowest convergence is in the spin- and isospin-independent part of the quasiparticle interaction F, which even up to $L = 9$ has contributions greater than 0.1. The Legendre polynomial expansion in all other channels is nearly converged by $L = 5$.

IV. CONCLUSIONS AND OUTLOOK

In the present work we have computed for the first time the full set of central and noncentral contributions to the quasiparticle interaction in symmetric nuclear matter up to twice nuclear saturation density. We have derived general formulas that allow one to extract the associated scalar functions from appropriate linear combinations of spin- and isospin-space matrix elements. Both two- and three-body forces are included at first and second order in perturbation theory, with the involved numerical calculations of the second-order diagrams benchmarked against model interactions. Three-body forces at the Hartree-Fock level are shown to give important contributions to the relative tensor and cross-vector interactions. Indeed, the isovector cross-vector interaction is dominated by three-body forces, in particular the two-pion exchange term proportional to the low-energy constant c_4, and only the second-order particle-hole diagram leads to a modest reduction of the strength in this channel. While the relative tensor force from the free-space nucleon-nucleon interaction is enhanced in the medium by three-body forces and second-order perturbative corrections, the center-of-mass tensor force remains relatively weak.

We have considered five different nuclear force models in order to estimate theoretical uncertainties. Up to nuclear saturation density, the relative tensor force in both the isoscalar and isovector channels is well constrained by microscopic many-body theory, which should be valuable for efforts to include effective tensor forces in mean-field modeling and density functional theory. In addition we find robust evidence for a strong isovector cross-vector interaction which is not normally included in mean-field models and may be important for spin-dependent phenomena. We benchmark the quality of our results against bulk nuclear matter properties, such as the incompressibility, isospin-asymmetry energy, and nucleon effective mass, which are directly related to selected central Fermi liquid parameters. While the theory uncertainties are sometimes large, in all cases the results are consistent with empirical constraints.

The present calculations are a step toward the microscopic description of response functions in nuclear matter consistent with equations of state exhibiting realistic nuclear saturation properties. In the future this work will be extended to isospin-asymmetric nuclear systems with applications to neutrino processes in neutron stars and supernovae.

ACKNOWLEDGMENTS

T.R.W. thanks S. Guha for informative discussions. Work was supported by the National Science Foundation under Grant No. PHY1652199. The work of N. Kaiser has been supported in part by DFG and NSFC through funds provided to the Sino-German CRC 110 "Symmetries and the Emergence of Structure in QCD." Portions of this research were conducted with the advanced computing resources provided by Texas A&M High Performance Research Computing.

APPENDIX: CENTRAL COMPONENTS OF THE QUASIPARTICLE INTERACTION FROM THE N2LO CHIRAL THREE-BODY FORCE

In this section we provide for completeness the central Fermi liquid parameters for arbitrary values of L resulting from the N2LO chiral three-body force. The various terms are organized according to the different topologies shown in Fig. 3. Some contributions are explicitly separated into a direct "d" and exchange "e" term. For notational convenience we introduce the abbreviations $\sigma = \vec{\sigma}_1 \cdot \vec{\sigma}_2$ and $\tau = \vec{\tau}_1 \cdot \vec{\tau}_2$. The contributions from the six topologies read

$$\mathcal{F}_L^{(\mathrm{med},1)} = (\sigma-3)(3-\tau)\frac{4g_A^2 m_\pi^3 u}{9\pi^2 f_\pi^4}\int_0^u dx\, x^3(2L+1)P_L(1-2x^2u^{-2})\,\frac{c_1+2c_3x^2}{(1+4x^2)^2}, \tag{A1}$$

$$\begin{aligned}\mathcal{F}_L^{(\mathrm{med},2)} &= (3-\sigma)(3-\tau)\frac{g_A^2 m_\pi^3}{(12\pi)^2 f_\pi^4 u^5}\int_0^u dx\,\frac{x^3(2L+1)}{1+4x^2}P_L(1-2x^2u^{-2})\Big\{16u^3(c_3-2c_4)\arctan 2u\\ &+\left[\frac{3x^2}{2}(c_3+c_4)(4+u^{-2})+6u^2(c_4-c_3-2c_1)-3c_1-\frac{c_3+c_4}{2}\right]\ln(1+4u^2)\\ &+2(c_3+c_4)x^2(8u^4-6u^2-3)+12c_1u^2(1+2u^2)+2c_3u^2\left(1-6u^2+\frac{8u^4}{3}\right)+2c_4u^2\left(1+18u^2-\frac{40u^4}{3}\right)\Big\},\end{aligned} \tag{A2}$$

$$\mathcal{F}_0^{(\mathrm{med},3\mathrm{d})} = \frac{g_A^2 m_\pi^3}{16\pi^2 f_\pi^4}\left\{24u(c_3-c_1)-8c_3u^3+6(6c_1-5c_3)\arctan 2u+\frac{3}{u}(3c_3-4c_1)\ln(1+4u^2)\right\}, \tag{A3}$$

$$\begin{aligned}\mathcal{F}_L^{(\mathrm{med},3\mathrm{e})} &= \frac{3g_A^2 m_\pi^3}{32\pi^3 f_\pi^4}\int_0^u dl\, l^2\int_{-1}^1 dx\int_{-1}^1 dy\int_0^\pi d\phi\,\frac{(2L+1)P_L(z)}{(1+u^2+l^2-2ulx)(1+u^2+l^2-2uly)}\\ &\times\Big\{(1+\sigma)(1+\tau)[2c_1(u^2z-ulx-uly+l^2)+c_3(u^2z-ulx-uly+l^2)^2]\\ &+(3-\sigma)(3-\tau)\frac{c_4}{9}[(u^2z-ulx-uly+l^2)^2-(u^2+l^2-2ulx)(u^2+l^2-2uly)]\Big\},\end{aligned} \tag{A4}$$

with $z = xy + \sqrt{(1-x^2)(1-y^2)}\cos\phi$,

$$\mathcal{F}_L^{(\mathrm{med},4)} = (3-\sigma)(3-\tau)\frac{g_A c_D m_\pi^3 u}{18\pi^2 f_\pi^4 \Lambda_\chi}\int_0^u dx\,\frac{x^3(2L+1)}{1+4x^2}P_L(1-2x^2u^{-2}), \tag{A5}$$

to which only the exchange term contributes,

$$\mathcal{F}_0^{(\mathrm{med},5)} = (3-\sigma-\tau-\sigma\tau)\frac{g_A c_D m_\pi^3}{16\pi^2 f_\pi^4 \Lambda_\chi}\left\{\frac{2u^3}{3} - u + \arctan 2u - \frac{1}{4u}\ln(1+4u^2)\right\}, \tag{A6}$$

$$\mathcal{F}_0^{(\mathrm{med},6)} = (\sigma+\tau+\sigma\tau-3)\frac{c_E k_f^3}{4\pi^2 f_\pi^4 \Lambda_\chi}. \tag{A7}$$

[1] L. D. Landau, Sov. Phys. JETP **3**, 920 (1957).
[2] L. D. Landau, Sov. Phys. JETP **5**, 101 (1957).
[3] L. D. Landau, Sov. Phys. JETP **8**, 70 (1959).
[4] A. B. Migdal and A. I. Larkin, Sov. Phys. JETP **18**, 717 (1964).
[5] G. E. Brown, Rev. Mod. Phys. **43**, 1 (1971).
[6] N. Iwamoto and C. J. Pethick, Phys. Rev. D **25**, 313 (1982).
[7] P. Haensel and A. J. Jerzak, Phys. Lett. **B112**, 285 (1982).
[8] S.-O. Bäckman, G. E. Brown, and J. A. Niskanen, Phys. Rep. **124**, 1 (1985).
[9] J. Wambach, T. L. Ainsworth, and D. Pines, Nucl. Phys. **555**, 128 (1993).
[10] B. Friman and M. Rho, Nucl. Phys. **A606**, 303 (1996).
[11] O. Benhar and M. Valli, Phys. Rev. Lett. **99**, 232501 (2007).
[12] A. Pastore, D. Davesne, Y. Lallouet, M. Martini, K. Bennaceur, and J. Meyer, Phys. Rev. C **85**, 054317 (2012).
[13] O. Benhar, A. Cipollone, and A. Loreti, Phys. Rev. C **87**, 014601 (2013).
[14] P. Haensel and J. Dabrowski, Nucl. Phys. **A254**, 211 (1975).
[15] A. Schwenk and B. Friman, Phys. Rev. Lett. **92**, 082501 (2004).
[16] E. Olsson, P. Haensel, and C. J. Pethick, Phys. Rev. C **70**, 025804 (2004).
[17] S. Bacca, K. Hally, C. J. Pethick, and A. Schwenk, Phys. Rev. C **80**, 032802(R) (2009).
[18] C. J. Pethick and A. Schwenk, Phys. Rev. C **80**, 055805 (2009).
[19] D. Davesne, J. W. Holt, A. Pastore, and J. Navarro, Phys. Rev. C **91**, 014323 (2015).
[20] L. F. Roberts, G. Shen, V. Cirigliano, J. A. Pons, S. Reddy, and S. E. Woosley, Phys. Rev. Lett. **108**, 061103 (2012).
[21] B. Bertoni, S. Reddy, and E. Rrapaj, Phys. Rev. C **91**, 025806 (2015).
[22] T. Otsuka, T. Suzuki, R. Fujimoto, H. Grawe, and Y. Akaishi, Phys. Rev. Lett. **95**, 232502 (2005).
[23] T. Otsuka, T. Matsuo, and D. Abe, Phys. Rev. Lett. **97**, 162501 (2006).
[24] B. Friman and P. Haensel, Phys. Lett. **B98**, 323 (1981).
[25] L.-G. Cao, G. Colò, H. Sagawa, P. F. Bortignon, and L. Sciacchitano, Phys. Rev. C **80**, 064304 (2009).
[26] G. Co', V. De Donno, M. Anguiano, and A. M. Lallena, Phys. Rev. C **85**, 034323 (2012).
[27] B. S. Pudliner, A. Smerzi, J. Carlson, V. R. Pandharipande, S. C. Pieper, and D. G. Ravenhall, Phys. Rev. Lett. **76**, 2416 (1996).
[28] B. A. Brown and A. Schwenk, Phys. Rev. C **89**, 011307 (2014).
[29] A. Roggero, A. Mukherjee, and F. Pederiva, Phys. Rev. C **92**, 054303 (2015).
[30] M. Buraczynski and A. Gezerlis, Phys. Rev. Lett. **116**, 152501 (2016).
[31] E. Rrapaj, A. Roggero, and J. W. Holt, Phys. Rev. C **93**, 065801 (2016).
[32] Z. Zhang, Y. Lim, J. W. Holt, and C.-M. Ko, Phys. Lett. B **777**, 73 (2018).
[33] T. Lesinski, M. Bender, K. Bennaceur, T. Duguet, and J. Meyer, Phys. Rev. C **76**, 014312 (2007).
[34] G. A. Lalazissis, S. Karatzikos, M. Serra, T. Otsuka, and P. Ring, Phys. Rev. C **80**, 041301(R) (2009).
[35] G. Colò, H. Sagawa, S. Fracasso, and P. F. Bortignon, Phys. Lett. B **646**, 227 (2007).
[36] W. Zou, G. Colò, Z. Ma, H. Sagawa, and P. F. Bortignon, Phys. Rev. C **77**, 014314 (2008).
[37] F. Minato and C. L. Bai, Phys. Rev. Lett. **110**, 122501 (2013).
[38] H. Sagawa and G. Colò, Prog. Part. Nucl. Phys. **76**, 76 (2014).
[39] G. E. Brown, S.-O. Bäckman, E. Oset, and W. Weise, Nucl. Phys. **A286**, 191 (1977).
[40] C. Shen, U. Lombardo, N. Van Giai, and W. Zuo, Phys. Rev. C **68**, 055802 (2003).
[41] W. Zuo, C. Shen, and U. Lombardo, Phys. Rev. C **67**, 037301 (2003).
[42] N. Kaiser, Nucl. Phys. **A768**, 99 (2006).
[43] D. Gambacurta, U. Lombardo, and W. Zuo, Phys. At. Nucl. **74**, 1424 (2011).
[44] J. W. Holt, N. Kaiser, and W. Weise, Nucl. Phys. **A876**, 61 (2012).
[45] J. W. Holt, N. Kaiser, and W. Weise, Phys. Rev. C **87**, 014338 (2013).
[46] D. R. Entem and R. Machleidt, Phys. Rev. C **68**, 041001 (2003).
[47] L. Coraggio, A. Covello, A. Gargano, N. Itaco, D. R. Entem, T. T. S. Kuo, and R. Machleidt, Phys. Rev. C **75**, 024311 (2007).
[48] E. Marji, A. Canul, Q. MacPherson, R. Winzer, C. Zeoli, D. R. Entem, and R. Machleidt, Phys. Rev. C **88**, 054002 (2013).
[49] L. Coraggio, J. W. Holt, N. Itaco, R. Machleidt, and F. Sammarruca, Phys. Rev. C **87**, 014322 (2013).
[50] L. Coraggio, J. W. Holt, N. Itaco, R. Machleidt, L. E. Marcucci, and F. Sammarruca, Phys. Rev. C **89**, 044321 (2014).
[51] F. Sammarruca, L. Coraggio, J. W. Holt, N. Itaco, R. Machleidt, and L. E. Marcucci, Phys. Rev. C **91**, 054311 (2015).
[52] S. Weinberg, Physica A **96**, 327 (1979).
[53] E. Epelbaum, H.-W. Hammer, and U.-G. Meißner, Rev. Mod. Phys. **81**, 1773 (2009).
[54] R. Machleidt and D. R. Entem, Phys. Rep. **503**, 1 (2011).
[55] V. Bernard, E. Epelbaum, H. Krebs, and U.-G. Meißner, Phys. Rev. C **77**, 064004 (2008).
[56] V. Bernard, E. Epelbaum, H. Krebs, and U.-G. Meißner, Phys. Rev. C **84**, 054001 (2011).

[57] I. Tews, T. Krüger, K. Hebeler, and A. Schwenk, Phys. Rev. Lett. **110**, 032504 (2013).
[58] C. Drischler, A. Carbone, K. Hebeler, and A. Schwenk, Phys. Rev. C **94**, 054307 (2016).
[59] C. Drischler, K. Hebeler, and A. Schwenk, arXiv:1710.08220.
[60] J. W. Holt and N. Kaiser, Phys. Rev. C **95**, 034326 (2017).
[61] C. Wellenhofer, J. W. Holt, N. Kaiser, and W. Weise, Phys. Rev. C **89**, 064009 (2014).
[62] J. W. Holt, N. Kaiser, G. A. Miller, and W. Weise, Phys. Rev. C **88**, 024614 (2013).
[63] J. W. Holt, N. Kaiser, and G. A. Miller, Phys. Rev. C **93**, 064603 (2016).
[64] J. W. Holt, N. Kaiser, and W. Weise, Nucl. Phys. **A870-871**, 1 (2011).
[65] J. W. Holt, N. Kaiser, and W. Weise, Phys. Rev. C **79**, 054331 (2009).
[66] J. W. Holt, N. Kaiser, and W. Weise, Phys. Rev. C **81**, 024002 (2010).
[67] S.-O. Bäckman, O. Sjöberg, and A. D. Jackson, Nucl. Phys. **A321**, 10 (1979).
[68] A. B. Migdal, *Theory of Finite Fermi Systems and Applications to Atomic Nuclei* (Interscience, New York, 1967).
[69] G. Baym and C. Pethick, *Landau Fermi-liquid Theory* (Wiley & Sons, New York, 1991).
[70] D. H. Youngblood, H. L. Clark, and Y.-W. Lui, Phys. Rev. Lett. **82**, 691 (1999).
[71] S. Shlomo, V. M. Kolomietz, and G. Colò, Eur. Phys. J. A **30**, 23 (2006).
[72] G. E. Brown, J. H. Gunn, and P. Gould, Nucl. Phys. **46**, 598 (1963).
[73] G. F. Bertsch and T. T. S. Kuo, Nucl. Phys. **A112**, 204 (1968).
[74] N. Kaiser, Phys. Rev. C **91**, 065201 (2015).
[75] C. Wellenhofer, J. W. Holt, and N. Kaiser, Phys. Rev. C **93**, 055802 (2016).
[76] G. Bertsch, D. Cha, and H. Toki, Phys. Rev. C **24**, 533 (1981).
[77] C. Gaarde, J. Rapaport, T. N. Taddeucci, C. D. Goodman, C. C. Foster, D. E. Bainum, C. A. Goulding, M. B. Greenfield, D. J. Horen, and E. Sugarbaker, Nucl. Phys. **A369**, 258 (1981).
[78] M. Bender, J. Dobaczewski, J. Engel, and W. Nazarewicz, Phys. Rev. C **65**, 054322 (2002).